International Journal on
"Technical and Physical Problems of Engineering"
(IJTPE)
Published by International Organization of IOTPE

ISSN 2077-3528
IJTPE Journal
www.iotpe.com
ijtpe@iotpe.com

June 2022 | Issue 51 | Volume 14 | Number 2 | Pages 27-35

NUMERICAL INVESTIGATION OF FREE VIBRATION FOR 3D PRINTED FUNCTIONALLY GRADED MATERIAL CANTILEVER BEAM

H.H. Mahdi S.A. Nama

Engineering Technical College of Baghdad, Middle Technical University, Baghdad, Iraq
dr_hassan1961@yahoo.com, drsami1959@gmail.com

Abstract- The increasing needs of the industry involved in development of components for aerospace and power sector demand the engineering community to develop new concepts and strategies to improve the functional requirements of structures and to enhance the strength of materials. This is particularly essential in the cases of rotating beams that are subjected to severe vibration under large pressure loadings, high rotating accelerations, centrifugal forces, geometric stiffening, etc. The current study aims to model a 3D printed functionally graded material beam with variable internal filling patterns along its longitudinal axis, and numerically investigate the effect of filling percentage and rotational speed on the fundamental frequency of a cantilever beam. The intent of this work focuses on the ability of using 3D printing process to print a functionally graded material beam and investigate the best distribution of internal ribs within the beam. The natural frequencies of 3D printed solid beam and proposed functionally graded beam were compared, it was observed that 3d printed functionally graded beam has higher natural frequencies than a solid beam subjected to same conditions like dimensions and rotational speeds. Results showed that the prestress has big effect on the fundamental frequency. An improvement of more than 33% in fundamental frequency can be obtained with functionally graded material beam compare with solid beam from same material.

Keywords: Beam Vibration, 3D Printing, Preload, FGM, Infill, Free Vibration.

1. INTRODUCTION

Helicopter blades, Centrifugal pump impellers, wind turbine blades are common applications for the high-speed rotating structures and can be made of plastics. Modal analysis is an important aspect when designing and optimizing rotating structures, it is used to determine the natural frequencies and mode shapes of these structures. These structures can be treated as cantilever beams; and during rotation, inertial forces developed and create stresses which in turn affects the natural frequencies and mode shapes of the cantilever rotating beam. Increasing the rotational speed increases the natural frequency due to the change in beam dynamic stiffness [1-3].

Plastic parts can be manufactured by Injection molding or subtractive manufacturing. In the first method, plastic is inserted into a mold to form the required object which will be either solid or an empty object. In subtractive manufacturing, material is removed from the workpiece stock and the object is completely solid. The 3D printing is an additive manufacturing process where different materials like Polylactic acid (PLA), Acrylonitrile butadiene styrene (ABS) polymers can be used to create mechanical parts, prototypes, domestic products rapidly by extruding the material in an adjustable fashion layer by layer to form the part using controlled density and pattern [4].

Recently, beams made of functionally graded materials (FGMs) are developed; they are beams with variable properties along their thickness or along the axial direction. They are used in applications like space vehicles and aircrafts. Many researches were conducted in the past decade to study the dynamic behavior of FGM beams using different analytical and numerical methods to analyze different beams with different end supporting conditions [5-13].

In 3D printing and for few cases, objects are printed as solid parts because they consume large amount of printing filament and take longer time to print, therefore they are costly. On the other hand, 3D printed hollow objects are cheaper because they need less material and printing time but they are unsuitable for many applications as they are not strong and fracture easily under stress. In 3D printing, one can control the two main regions in the part: the external region (perimeter or wall) and the internal region within the part (Infill). Infill is the internal structure of the printed object; it is used to strengthen the hollow part and significantly affects its weight and flexibility.

In 3D printed objects are influenced by different parameters like infill density, filling pattern, print speed, printing material, print temperature, and nozzle diameter [14, 15, 16]. Increasing infill density increases the tensile strength, the compressive strength and elastic modulus; on the other hand, increasing the infill density increases the printing time [17-21].

Infill patterns can be rectilinear, honeycomb, triangles, concentric, line, and other shape patterns. The complexity of filling pattern affects the printing time, increasing the number of perimeter shells may increase the strength and stiffness of the printed part, while increasing the layer thickness increases the mechanical strength [22-24]. The current work aims to investigate the effect of stress stiffening caused by the rotational speed on the fundamental frequency of a cantilever 3D printed beam using the numerical method. To obtain a functionally graded material beam, its inner part was filled with different manners.

2. THEORY

For beam element, the stiffness matrix for the first element is [25]:

$$[K_1]=\frac{E}{L^2}\begin{bmatrix} 12I_1 & 6LI_1 & -12I_1 & 6LI_1 \\ 6LI_1 & 4L^2I_1 & -6LI_1 & 2L^2I_1 \\ -12I_1 & -6LI_1 & 12I_1 & -6LI_1 \\ 6LI_1 & 2L^2I_1 & -6LI_1 & 4L^2I_1 \end{bmatrix} \quad (1)$$

and the consistent mass matrix for this element is:

$$[M_1]=\frac{\rho L}{420}\begin{bmatrix} 156A_1 & 22LA_1 & 54A_1 & -13LA_1 \\ 22LA_1 & 4L^2A_1 & 13LA_1 & -3L^2A_1 \\ 54A_1 & 13LA_1 & 156A_1 & -22LA_1 \\ -13LA_1 & -3L^2A_1 & -22LA_1 & 4L^2A_1 \end{bmatrix} \quad (2)$$

where,

E = Young's modulus (N/mm^2)

I = Moment of inertia (mm^4)

L = length (mm)

ρ = weight density (N/m^3)

A = Area (mm^2)

The stiffness matrix for the second element is:

$$[K_2]=\frac{E}{L^2}\begin{bmatrix} 12I_2 & 6LI_2 & -12I_2 & 6LI_2 \\ 6LI_2 & 4L^2I_2 & -6LI_2 & 2L^2I_2 \\ -12I_2 & -6LI_2 & 12I_2 & -6LI_2 \\ 6LI_2 & 2L^2I_2 & -6LI_2 & 4L^2I_2 \end{bmatrix} \quad (3)$$

and the consistent mass matrix is:

$$[M_2]=\frac{\rho L}{420}\begin{bmatrix} 156A_2 & 22LA_2 & 54A_2 & -13LA_2 \\ 22LA_2 & 4L^2A_2 & 13LA_2 & -3L^2A_2 \\ 54A_2 & 13LA_2 & 156A_2 & -22LA_2 \\ -13LA_2 & -3L^2A_2 & -22LA_2 & 4L^2A_2 \end{bmatrix} \quad (4)$$

The assembled stiffness matrix will be

$$[K]=\frac{E}{L^3}$$

$$\begin{bmatrix} 12I_1 & 6LI_1 & -12I_1 & 6LI_1 & 0 & 0 \\ 6LI_1 & 4L^2I_1 & -6LI_1 & 2L^2I_1 & 0 & 0 \\ -12I_1 & -6LI_1 & 12I_1+12I_2 & -6LI_1+6LI_2 & -12LI_2 & 6LI_2 \\ 6LI_1 & 2L^2I_1 & -6LI_1+6LI_2 & 4L^2I_1+4L^2I_2 & -6LI_2 & 2L^2I_2 \\ 0 & 0 & -12I_2 & -6LI_2 & 12I_2 & -6LI_2 \\ 0 & 0 & 6LI_2 & 2L^2I_2 & -6LI_2 & 4L^2I_2 \end{bmatrix} \quad (5)$$

and the assembled mass matrix:

$$[M]=\frac{\rho L}{420}$$

$$\begin{bmatrix} 156A_1 & 22LA_1 & 54A_1 & -13LA_1 & 0 & 0 \\ 22LA_1 & 4L^2A_1 & 13LA_1 & -3L^2A_1 & 0 & 0 \\ 54A_1 & 13LA_2 & 156A_1+156A_2 & -22LA_1+22LA_2 & 54A_2 & -13LA_2 \\ -13LA_1 & -3L^2A_1 & -22LA_1+22LA_2 & 4L^2A_1+4L^2A_2 & 13LA_2 & -3L^2A_2 \\ 0 & 0 & 54A_2 & 13LA_2 & 156A_2 & -22LA_2 \\ 0 & 0 & -13LA_2 & -3L^2A_2 & -22LA_2 & 4L^2A_2 \end{bmatrix} \quad (6)$$

The global matrix is:

$$\left\{[K]-\omega^2[M]\right\}\{n\} \quad (7)$$

where, n is the number of elements.

Substituting Equations (5) and (6) in Equation (7) and equating the determinant of the resulting matrix to zero will yields to the natural frequencies of the beam. It is obvious that increasing the number of elements and using assigning different moment of inertia and cross section area for each element will complicate the analytical solution. Therefore, it is common to obtain the solution by using the numerical approach.

The exact solution for a solid cantilever beam is given by [25]:

$$\omega_1=1.8751^2\sqrt{\frac{EI}{\rho AL^4}} \quad (8)$$

3. NUMERICAL MODELING

A cantilever beam made of Acrylonitrile butadiene styrene (ABS) thermoplastic was modeled in Solid works 2018. The beam was 400 mm long, 30 mm wide and 5 mm thick. The ABS properties were (Elastic Modulus = 2000 MPa, Poisson's ratio = 0.394, Mass Density = 1020 Kg/m^3). Solid element was used to mesh the beam with element size equals 2.2 mm which gives 67167 nodes and 33859 elements. To obtain the cantilever boundary conditions, the beam was fixed at one end and free at the other end as shown in Figure 1.

To study the effect of internal filling pattern on the fundamental frequency, different beams were modeled with different parameters (wall thickness, rib thickness, rib location, rib number and rib length). For each model, three rotational speeds (2000, 2500 and 3000 rpm) were applied to the beam and the effect of the gravity as an applied load was taken in consideration to find out the effect of preload on the fundamental frequency.

The 3D printed hollow beam is considered as it is consisted of three parts, a frame that is 3mm height, a base with 1mm thickness, and a cover with 1mm thickness as shown in Figure 2. The beam is fixed at one end and free at the other end. For each beam, the mass was obtained and converted into a corresponding infill percentage according to Equation (9).

$$\text{Infill}\,\% = \frac{\text{New beam mass}}{\text{Original solid beam mass}} \times 100 \quad (9)$$

Figure 1. ABS cantilever beam model

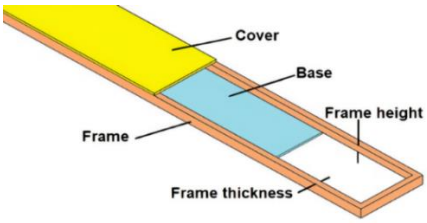

Figure 2. 3D printed hollow beam

4. RESULTS AND DISCUSSIONS

4.1. Case 1: Solid Model 100% Infill

For the solid cantilever beam in its stationary state, the mass was 61.277 grams i.e., Infill = 100%, and the first five natural frequencies were 7.1106, 42.107, 44.52, 124.57, and 165.56 Hz, respectively, these frequencies are in best agreement with the exact results given in Equation (8) [25]. The mode shape of these frequencies is shown in Figure 3. We will consider the fundamental frequency as it is the most important one. When applying the three different rotational speeds, the resulting natural frequencies, stresses, and beam deflections are listed in Table 1.

Table 1. Variation of fundamental frequency, stress and deflection at different beam speeds

	Rotation Speed (RPM)		
	2000	2500	3000
f_1 (Hz)	39.796	49.193	58.583
Stress (N/mm^2)	7.908	12.205	17.459
Deflection (mm)	7.626	7.664	7.732

Comparing the results for the stationary and rotating beams, we can notice a strong effect of rotation speed on the frequency (when the beam rotates at 2000 rpm, its fundamental frequency increases in about six times its value for the stopped beam, i.e., from 7.1106 Hz to 39.796 Hz). The centrifugal force caused by rotation produces tensile stress in the beam which in turn leads to beam stress stiffening. For the rotating beam, the resultant stiffness is the sum of the stress stiffness and the beam elastic stiffness. The tensile stress produces positive stress stiffness; therefore, the resultant stiffness for the rotating beam is higher than that of the stopped one.

Increasing the beam stiffness, in turn, increases the beam natural frequency. Increasing the rotational speed increases the inertial effects and in turn increases the stresses created in the beam which results in more increment in the beam natural frequencies and mode shapes.

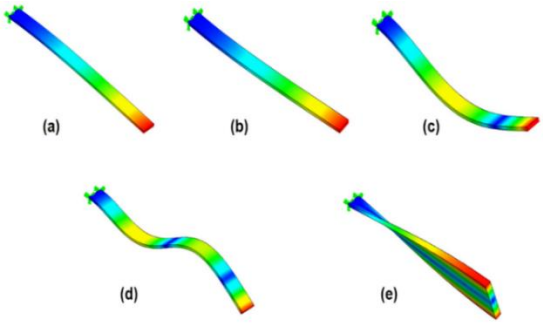

Figure 3. First five mode shapes for the solid cantilever beam

4.2. Case 2: Effect of Wall Thickness

In this case, five different frame wall thicknesses were considered 2.5, 5, 7.5, 10, and 12.5 mm. For each wall thickness the beam mass was obtained and converted into a corresponding infill percentage according to Equation (8). The effect of changing wall thickness on the fundamental frequency for the stationary beam is shown in Figure 4 and the effect of this change on mass, and beam infill percentage is listed in Table 2.

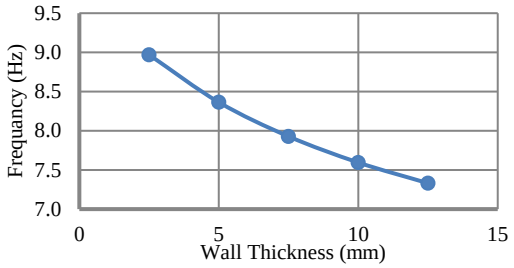

Figure 4. Effect of wall thickness on fundamental frequency for stationary beam

Table 2. Variation of mass and infill percentage with wall thickness for stationary beam

Wall thickness (mm)	2.5	5	7.5	10	12.5
Mass (gm)	31.02	37.37	43.56	49.61	55.5
Infill (%)	50.7	61.0	71.2	81.0	90.6

It can be noted from Figure 4 that increasing wall thickness decreases the fundamental frequency, this is due to the increase in the mass of the beam. The best result for this frequency was (8.97 Hz) which was achieved at 2.5 mm wall thickness. It can be concluded that decreasing the mass to 50.7% from the original beam mass provides an improvement in the fundamental frequency which equals (26%).

For each thickness, the beam was subjected to the rotational speeds (2000, 2500, and 3000 rpm). Figure 5 showed that stress and deflection are affected by wall thickness and rotational speed. Increasing wall thickness increases the mass of the beam and in turn increases the centrifugal force and tensile stress.

When the beam is subjected to different rotational speeds, the fundamental frequency is inversely affected by the wall thickness and directly influenced by the rotational speed as shown in Figure 6. A wall thickness of 2.5 mm was chosen for the printed beam because it gives the lowest stress, lowest deflection and the highest frequency.

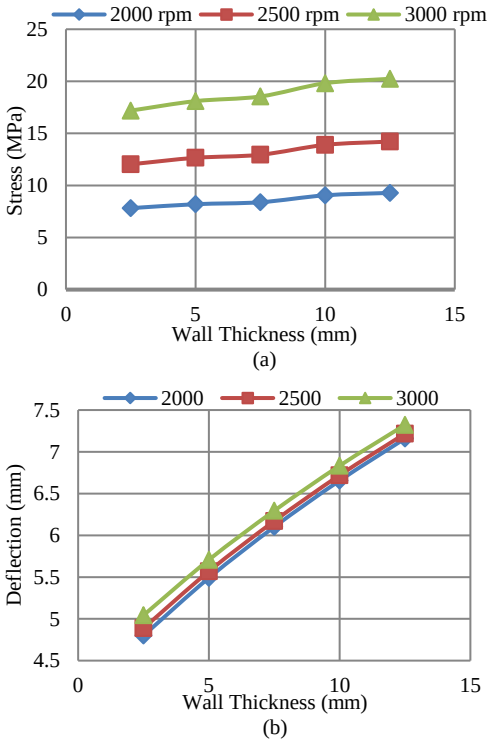

Figure 5. Effect of wall thickness for hollow beam at different rotational speeds (a) Stress and (b) Deflection

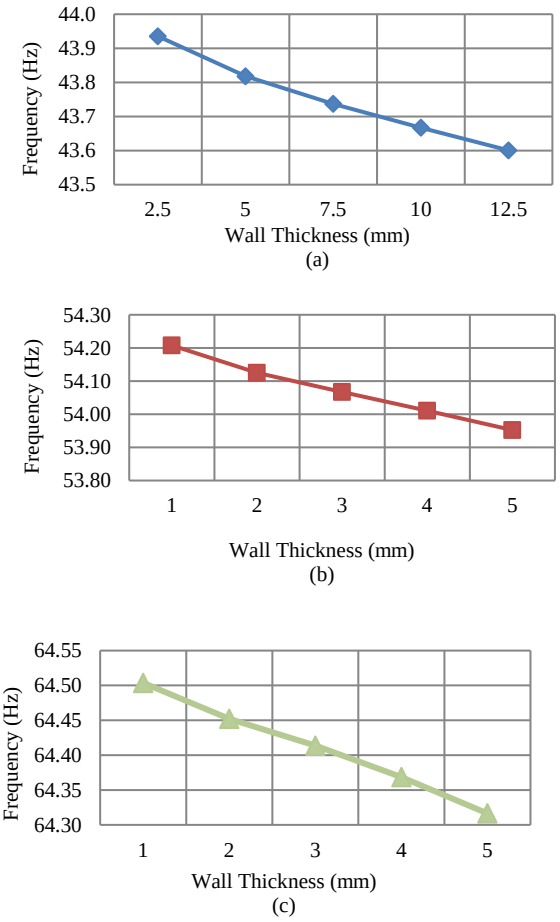

Figure 6. Effect of wall thickness on fundamental frequency for rotating beam at (a) 2000 RPM, (b) 2500 RPM and (c) 3000 RPM

4.3. Case 3: Effect of Rib Thickness

A transverse rib was added in this case at the mid length of the beam, its height was 3mm and thickness varies between 1.25 mm and 6.25 mm (step 1.25 mm). For not rotating beam, increasing the transverse rib thickness increases the mass of the beam therefore the fundamental frequency decreases as shown in Figure 7. The beast frequency value was 8.96 Hz which was obtained at 2.5 mm rib thickness. The mass of the beam becomes 31.212 grams, i.e., 50.94% infill.

For the rotating beams, it was noted that increasing rib thickness and rotational speed increases the stress and beam deflection as shown in Figure 8. Also, increasing rib thickness and rotational speed increases the frequency as listed in Table 3. The increase in frequency due to thickness change is so small and it can be considered constant, so that we can conclude that increasing rib thickness has no effect on frequency. We will choose 2.5 mm as rib thickness because it gives the lowest stress, lowest deflection and the highest frequency.

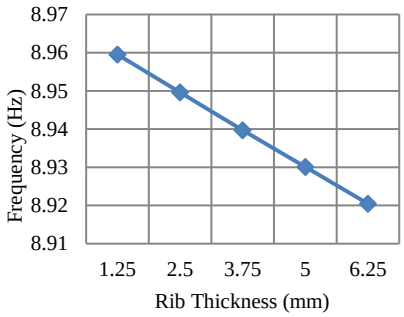

Figure 7. Effect of rib thickness on fundamental frequency for stationary beam

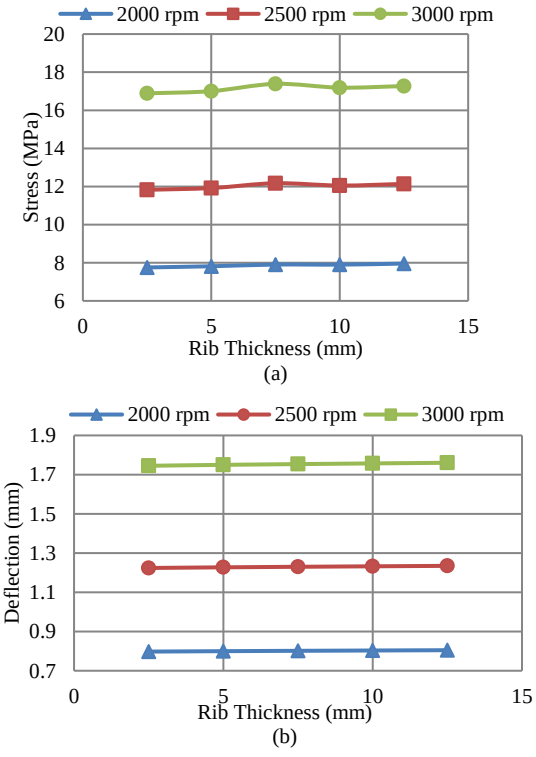

Figure 8. Effect of rib thickness at different speeds on (a) Stress and (b) deflection

Table 3. Variation of fundamental frequency with rib thickness at different speeds

rpm	Rib thickness (mm)				
	2.5	5	7.5	10	12.5
2000	43.944	43.951	43.959	43.967	43.974
2500	54.219	54.230	54.240	54.251	54.262
3000	64.518	64.532	64.545	64.560	64.573

4.4. Case 4: Effect of Rib Location

For this case the transverse rib will be located at different places away from the fixed edge of the beam, the mass of this beam remains constant 31.212 gm.

For the stationary beam, increasing rib distance decreases the fundamental frequency as shown in Figure 9. The best rib location is at distance 3.75 mm from the fixed edge which results in a 2.5 mm gap between the rib and the fixed edge, these results in a fundamental frequency equal 8.998 Hz.

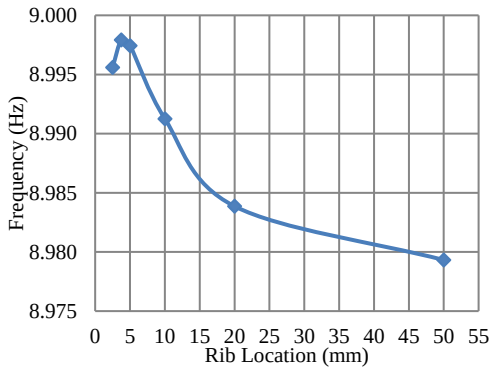

Figure 9. Effect of transverse rib location on fundamental frequency for stationary beam

For the rotating beams, increasing rib location decreases the stress and increases the deflection, while increasing the rotational speed increases both the stress and beam deflection as listed in Tables 4 and 5, respectively. The variation of the fundamental frequency with rib location at different rotational speeds is shown in Figure 10. It can be noted that increasing rib distance from the fixed edge decreases the frequency, the transverse rib acts as an added mass to the beam, and increasing rotational speed increases the frequency. The best frequency results were 44.00, 54.292, 64.609 Hz which were obtained at 2000, 2500, and 3000 rpm, respectively.

Table 4. Variation of stress with rib location at different rpm

rpm	Rib location (mm)					
	2.5	3.75	5	10	20	50
2000	9.611	8.710	8.251	7.617	7.723	7.737
2500	14.75	13.40	12.69	11.72	11.89	11.80
3000	21.03	19.13	18.12	16.75	16.99	16.84

Table 5. Variation of deflection with rib location at different rpm

rpm	Rib location (mm)					
	2.5	3.75	5	10	20	50
2000	4.77	4.77	4.77	4.77	4.78	4.79
2500	4.87	4.86	4.859	4.866	4.870	4.883
3000	5.028	5.02	5.015	5.021	5.023	5.039

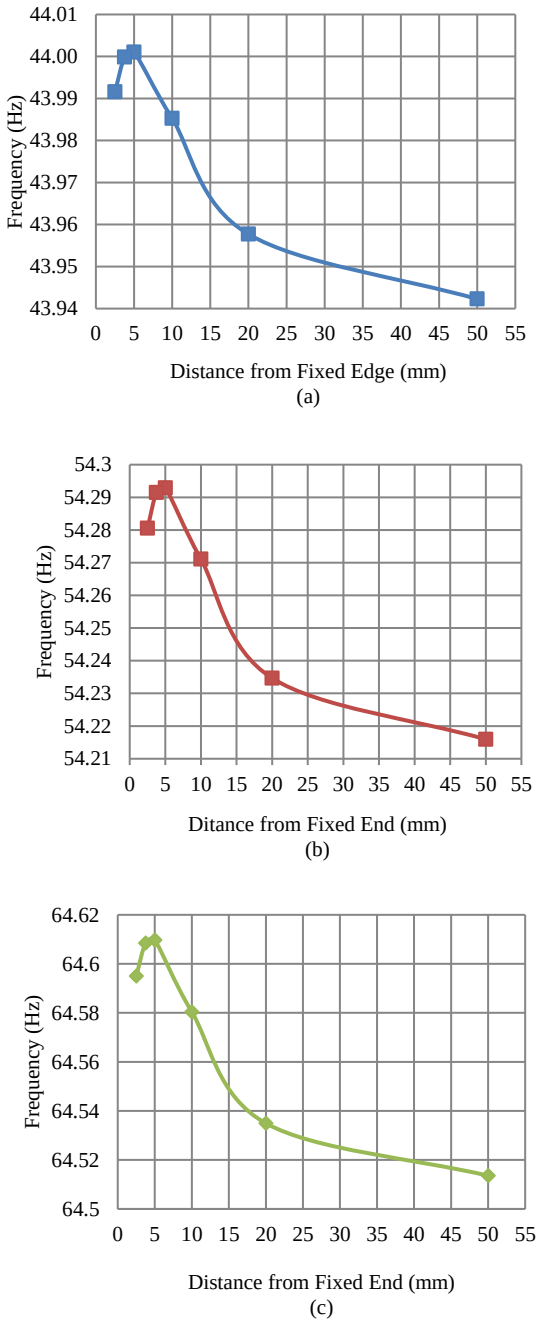

Figure 10. Effect of rib location on fundamental frequency for rotating beam at (a) 2000 rpm, (b) 2500 rpm and (c) 3000 rpm

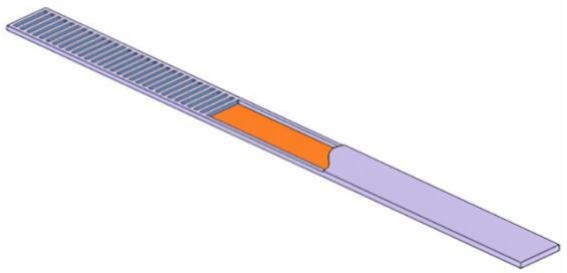

Figure 11. Hollow beam with transverse ribs

4.5. Case 5: Effect of Rib Number

In this case, multiple transverse ribs were added to the beam, each rib is 2.5 mm thickness and the distance between the ribs is 2.5 mm too as shown in Figure 11.

For the stationary beam, it was noted that increasing the number of ribs increases the fundamental frequency up to a maximum value then the frequency decreases as shown in Figure 12. The best number of ribs was 30 which results in a fundamental frequency equal 9.24 Hz. The resulting mass was 36.758 grams, i.e., 59.99% infill.

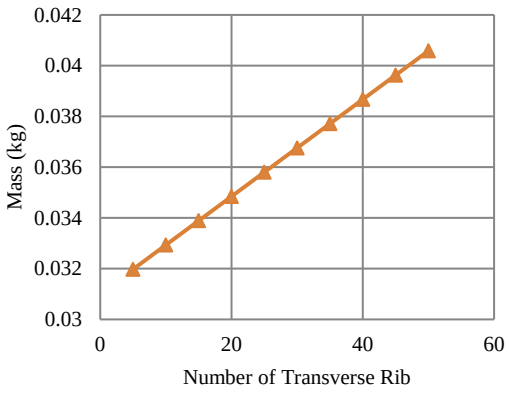

Figure 12. Effect of rib number on fundamental frequency for stationary beam

When the beam is subjected to different rotational speeds, the variation of stress and deflection is shown in Figure 13. It can be noted that stress and deflection are directly affected by increasing the number of transverse ribs and the rotational speed.

Increasing rib number and rotational speed increases the frequency as shown in Figure 14. Increasing rib number increases the inertia forces due to the increase in mass of the beam. 30 transverse ribs were considered as they give the best fundamental frequency for the stationary beam. For this number of ribs, the resulting frequency were 44.328, 54.699, 65.099 Hz for 2000, 2500 and 3000 rpm, respectively.

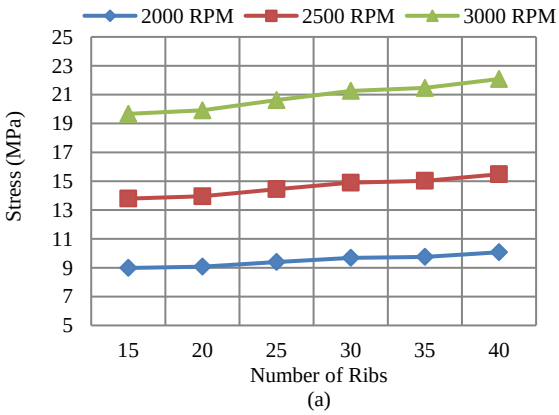

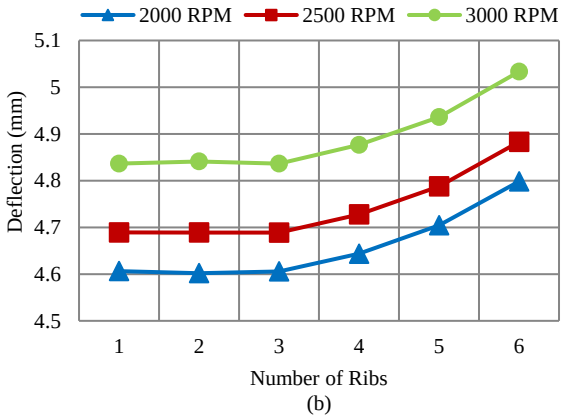

Figure 13. Effect of transverse rib number at different speeds on (a) Stress and (b) Deflection

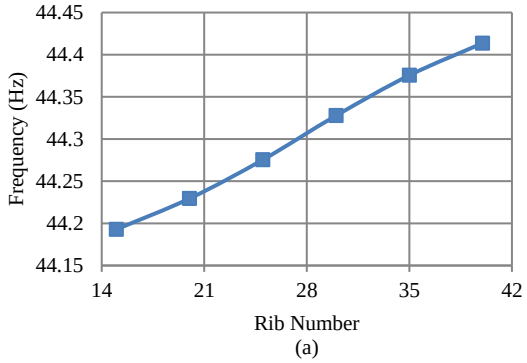

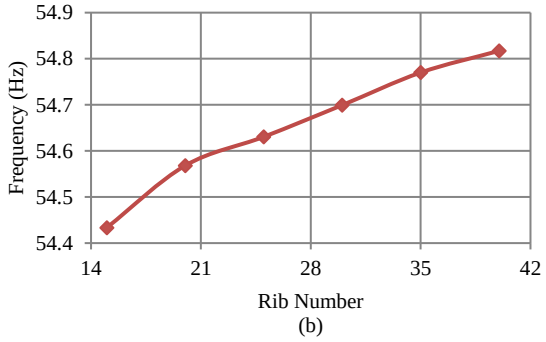

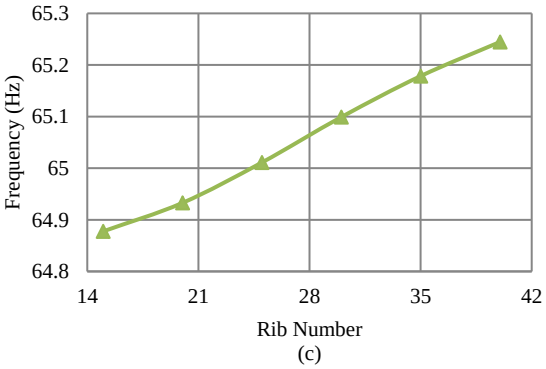

Figure 14. Effect of rib thickness on fundamental frequency for rotating beam (a) 2000 rpm, (b) 2500 rpm and (c) 3000 rpm

4.6. Case 6: Effect of Longitudinal Ribs Length

In this case, the beam contains 30 transverse ribs and five longitudinal ribs. The longitudinal ribs are 2.5 mm thickness with a distance of 2.5 mm between them and variable length as shown in Figure 15.

For stationary beam, increasing the rib length up to 150 mm increases the fundamental frequency up to 9.49 Hz then the frequency decreases with increasing the rib length as shown in Figure 16. The frequency is affected by both the mass and beam stiffness, therefore when the rib length is less than 150 mm, the frequency increases due to increase in beam stiffness while for longer beams the decrease in frequency is due to increase in beam mass. Adding five 150 mm longitudinal ribs improves the fundamental frequency by 33.45%, the corresponding beam mass is 39.627 grams, i.e., 64.65% infill.

The effect of rotating speed on stress and deflection is shown in Figure 17. It can be noted that the rib length of 150 mm results in the minimum stress.

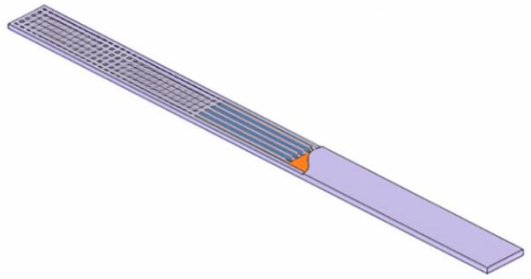

Figure 15. Hollow beam with longitudinal ribs

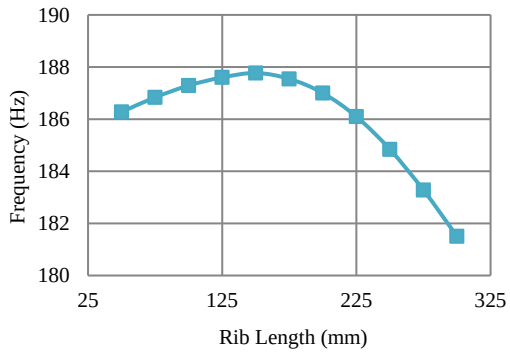

Figure 16. Effect of longitudinal rib length on fundamental frequency for stationary beam

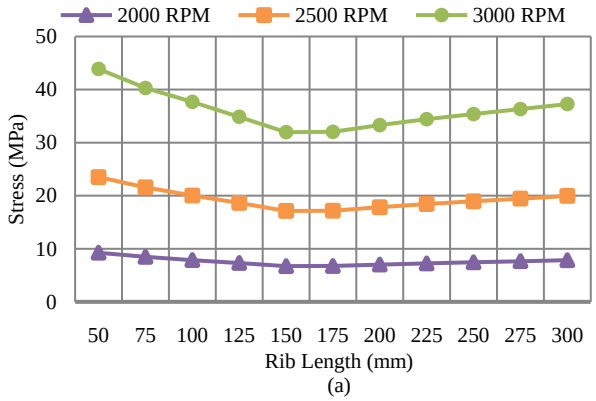

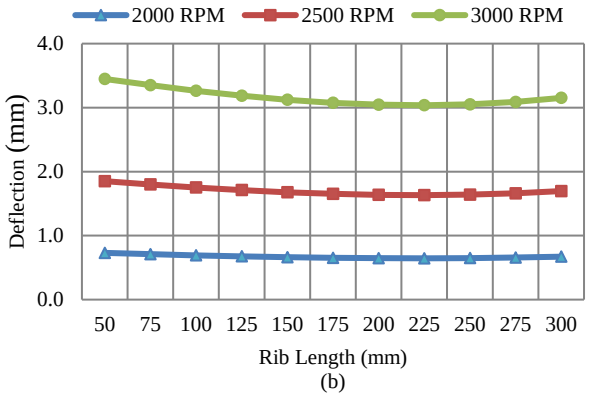

Figure 17. Effect of longitudinal rib length on (a) stress (b) deflection at different speeds

The fundamental frequency is directly influenced by both rib length and rotational speed as shown in Figure 18. The rib length 150 mm was considered, the resulting frequencies were 44.51, 54.85, 65.35 Hz for 2000, 2500 and 3000 rpm, respectively.

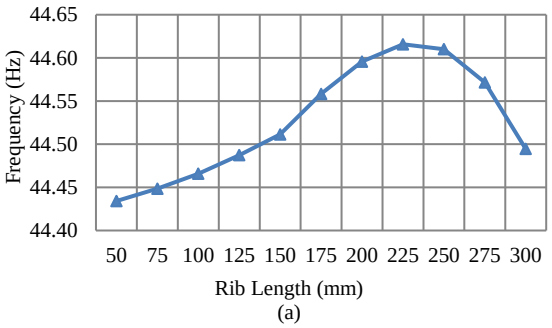

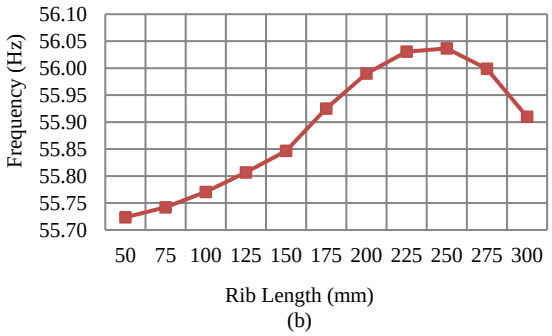

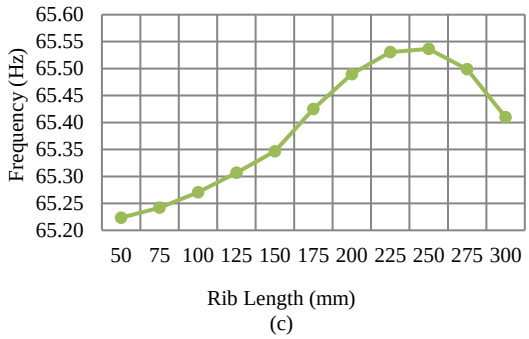

Figure 18. Effect of rib length on fundamental frequency for rotating beam (a) 2000 rpm, (b) 2500 rpm and (c) 3000 rpm

5. CONCLUSIONS

In the present work, cantilever 3D printed beams were numerically modelled by using SolidWorks as the finite element analysis software. Acrylonitrile butadiene styrene (ABS) thermoplastic was employed to conduct the modeled. The novelty of this study highlights the ability of using 3D printing process effectively to print a functionally graded material beam by adding internal ribs in certain distribution to the hollow beam. Adding the ribs increases the natural frequencies of the FGM beam in comparison with solid beam having the same material and dimensions

The results show that for hollow printed beam, increasing wall thickness increases the mass of the beam and therefore decreases its fundamental frequency. Increasing the rotational speed increases the pre-stresses created in the beam, this increases the beam natural frequencies and mode shapes. The transverse rib acts as an added mass to the beam, moving it away from the fixed edge decreases the fundamental frequency. Although increasing the number of transverse ribs increases the mass of the beam but it increases the inertia forces and in turn increases the fundamental frequency. Adding additional longitudinal ribs to a portion of the hollow beam will turn it into a functionally graded material beam. Although adding ribs increases the mass of the printed hollow beam up to 39.627 grams which represents 64.65% infill, the fundamental frequency can be improved by 33.45% compared with the solid beam

REFERENCES

[1] P. Pavelka, R. Hunady, M. Hagara, "The Influence of Preload on Modal Parameters of a Cantilever Beam", American Journal of Mechanical Engineering, Vol. 4, No. 7, pp. 418-422, 2016.

[2] S. Sendilvela, M. Prabhahar, "Pre-Stress Modal Analysis of a Centrifugal Pump Impeller for Different Blade Thicknesses", International Journal of Mechanical and Production Engineering, Research and Development (IJMPERD), Vol. 7, No. 6, pp. 507-516, 2017.

[3] M. Marzuki, M. Azmi, A. Mohamed, M. Balar, M. Nawi, "Pre-Stress Modal Analysis of Space Frame Chassis Structure Using Finite Element Method", International Journal of Engineering & Technology, Vol. 7, No. 4.36, pp. 1545-1548, 2018.

[4] S. Kannan, M. Ramamoorthy, "Mechanical Characterization and Experimental Modal Analysis of 3D Printed ABS, PC and PC-ABS Materials", Material Research Express, Vol. 7, No. 1, 2020.

[5] A.A. Khan, M.N. Alma, N. Rahman, M. Wajid, "Finite Element Modeling for Static and Free Vibration Response of Functionally Graded Beam", Latin American Journal of Solids and Structures, Vol. 13, No. 4, pp. 690-714, 2016.

[6] M. Avcar, H.H. Alwan, "Free Vibration of Functionally Graded Rayleigh Beam", International Journal of Engineering & Applied Sciences, Vol. 9, No. 2, pp. 127-127, 2017.

[7] K. Celebi, D. Yarimpabuc, N. Tutuncu, "Free Vibration Analysis of Functionally Graded Beams using Complementary Functions Method", Archive of Applied Mechanics, Vol. 88, No. 1-2, pp. 729-739, 2018.

[8] P. Kumar, K. Rao, N. Rao, "Effect of Taper on Free Vibration of Functionally Graded Rotating Beam by Mori-Tanaka Method", Journal of Institution of Engineers, Series C100, pp. 729-736, India, 2018.

[9] M. Mahmoud, "Natural Frequency of Axially Functionally Graded, Tapered Cantilever Beams with Tip Mass", Engineering Structures, Vol. 187, pp. 34-42, 2019.

[10] M. Bouamama, A. Elemeiche, A. Elhennani, T. Kebir, Z. Ei, "Exact Solution for Free Vibration Analysis of FGM Beams", Journal of Composite and advanced Materials, Vol. 2, No. 2, pp. 55-60, 2020.

[11] G. Sinha, B. Kumar, "Review on Vibration Analysis of Functionally Graded Material Structural Components with Cracks", Journal of Vibration Engineering & Technologies, Exact Solution for Free Vibration Analysis of FGM Beams", Vol. 9, pp. 23-49, 2020.

[12] S. Shabani, Y. Cunedioglu, "Free Vibration Analysis of Functionally Graded Beams with Cracks", Journal of Applied and Computational Mechanics, Issue 4, Vol. 6, pp. 908-919, 2020.

[13] Q. Atiyah, I. Abdulsahib, "Vibrations Analysis of Functionally Graded Beams at Different Boundary Conditions", Journal of Mechanical Engineering Research and Developments, Vol. 44, No. 3, pp. 181-188, 2021.

[14] N. Tho, T. Minh, N. Tai, "The Effect of Infill Pattern, Infill Density, Printing Speed and Temperature on the Additive Manufacturing Process Based on the FDM Technology for the Hook-Shaped Components", Journal of Polimesin, Vol. 18, No. 1, 2020.

[15] M. Lalegani, M. Ariffin, "The Effects of Combined Infill Patterns on Mechanical Properties in FDM Process", Journal of Polymers MPDI, Vol. 12, No. 12, pp. 2792, 2020.

[16] F.E. Nouman, S.A. Nama, H.H. Mahdi, "Effect of Infill Percentage for 3D Printed Dies on Spring Back for Aluminum Sheets", International Journal on Technical and Physical Problems of Engineering (IJTPE), Issue 49, Vol. 13, No. 4, pp. 27-32, December 2021.

[17] M. Fernandez-Vicente, W. Caile, S. Ferrandiz, A. Conejero, "Effect of Infill Parameters on Tensile Mechanical Behavior in Desktop 3D Printing", 3D Printing and Additive Manufacturing, Issue 3, Vol. 3, pp. 183-192, 2016.

[18] D. Patel, "Effects of Infill Patterns on Time, Surface Roughness and Tensile Strength in 3D Printing". International Journal of Engineering Development and Research, Vol. 5, No. 3, 2017.

[19] C. Lubombo, M. Huneault, "Effect of Infill Patterns on the Mechanical Performance of Lightweight 3D-Printed Cellular PLA Parts", Journal of Materials Today Communications, Vol. 17, pp. 214-228, 2018.

[20] A. Baig, K. Moeed, M. Haque, "A Study on the Effect of Infill Percentage and Infill Pattern on the Compressive Behavior of the FDM Printed Polylactic Acid (PLA) Polymer", Global Research and Development Journal for Engineering, Issue 9, Vol. 4, 2019.

[21] M. Rismalia, S. Hidajat, G. Permana, B. Hadisujoto, M. Muslimin, F. Triawan, "Infill Pattern and Density Effects on the Tensile Properties of 3D Printed PLA Material", Journal of Physics, Conference Series 1402, Issue 4, pp. 1-6, 2019.
[22] E. Cho, H. Hein, Z. Lynn, T. Tran, S. Hla, "Investigation on Influence of Infill Pattern and Layer Thickness on Mechanical Strength of PLA Material in 3D Printing Technology", Journal of Engineering and Science Research, Vol. 3, No. 2, pp. 27-37, 2019.
[23] M. Derise1, A. Zulkharnain, "Effect of Infill Pattern and Density on Tensile Properties of 3D Printed Polylactic acid Parts via Fused Deposition Modeling (FDM)", International Journal of Mechanical and Mechatronics Engineering IJMME-IJENS, Vol. 20, No. 2, 2020.
[24] Q. Ma, M. Rejab, A.P. Kumar, H. Fu, N.M. Kumer, J. Tang, "Effect of Infill Pattern, Density and Material Type of 3D Printed Cubic Structure under Quasi-Static Loading", Journal of Mechanical Engineering Science, Vol. 1, No. 1, pp. 1-19, 2020.
[25] S. Rao, "Vibration of Continuous Systems", John Wiley and Sons Inc., 2007.

BIOGRAPHIES

Hassan Hamoodi Mahdi was born in Baghdad, Iraq in July 1961. He obtained the Ph.D. degree in mechanical engineering / vibration from Hatfield Polytechnic, England in 1991. He is an Assistant Professor in the field of mechanical engineering in Department of Applied Mechanics, Technical Engineering College of Baghdad, Middle Technical University, Baghdad, Iraq. He had published 12 papers. His scientific interests are sound and vibrations, die and tools, materials and welding.

Sami Ali Nama was born in Baghdad, Iraq in August 1959. He received the M.Sc. degree in production engineering from University of Technology, Baghdad, Iraq in 1986. He also received the Ph.D. degree in mechanical engineering from the same university in 2010. He is a Professor in the field of mechanics and tool design in Department of Applied Mechanics, Technical Engineering College of Baghdad, Middle Technical University, Baghdad, Iraq. He had published 21 papers and two books. His scientific interests are, plate vibration, mechanics of materials, solid state mechanics, sheet metal forming.